

# Supplementary material

## Enantioseparation of ofloxacin using a liquid-liquid extraction system based on hydrophobic eutectic solvents

Mahtab Moradi<sup>1,2</sup>, Ana M. Ferreira<sup>1\*</sup>, Catarina M. S. S. Neves<sup>1</sup>, Filipe H. B. Sosa,<sup>1</sup> Gholamreza Pazuki<sup>2\*</sup> and João A.P. Coutinho<sup>1</sup>

<sup>1</sup>CICECO – Aveiro Institute of Materials, Department of Chemistry, University of Aveiro (UA), 3810-193 Aveiro, Portugal.

<sup>2</sup>Department of Chemical Engineering, Amirkabir University of Technology (Tehran Polytechnic), 1591634311 Tehran, Iran.

Corresponding author\*: Ana M. Ferreira (ana.conceicao@ua.pt); Gholamreza Pazuki (ghpazuki@aut.ac.ir)

## Tables

**Table S1.**  $2^3$  factorial planning - central composite rotatable design (CCRD).

Run	Coded variables		
	X <sub>1</sub>	X <sub>2</sub>	X <sub>3</sub>
1	-1	-1	-1
2	1	-1	-1
3	-1	1	-1
4	1	1	-1
5	-1	-1	1
6	1	-1	1
7	-1	1	1
8	1	1	1
9	-1.68	0	0
10	1.68	0	0
11	0	-1.68	0
12	0	1.68	0
13	0	0	-1.68
14	0	0	1.68
15	0	0	0
16	0	0	0
17	0	0	0
18	0	0	0
19	0	0	0
20	0	0	0

**Table S2.** Coded levels of independent variables used in the factorial planning - central composite rotatable design (CCRD).

Independent variables	Axial	Factorial	Central	Factorial	Axial
	-1.682	-1	0	1	1.682
<b>X<sub>1</sub> - pH</b>	3	3	4	5	5
<b>X<sub>2</sub> - Excess of chiral selector (CS)</b>	19.5	40.0	70.0	100.0	120.5
<b>X<sub>3</sub> - HES-water ratio (v/v)</b>	0.5	0.9	1.3	1.8	2.1

**Table S3.** Values of interaction energies, including hydrogen bonding (H-bond), electrostatic misfit (misfit), and van der Waals forces (vdW), calculated using COSMO-RS for aqueous mixtures of  $\beta$ -CD, S- $\beta$ -CD, or CM- $\beta$ -CD with OFX in either its zwitterionic or positive form, at 20-fold and 120-fold excess of the chiral selector.

Energy (kcal/mol)	Zwitterionic OFX					Positive OFX
	20x			120x		120x
	$\beta$ -CD	CM- $\beta$ -CD	S- $\beta$ -CD	CM- $\beta$ -CD	S- $\beta$ -CD	S- $\beta$ -CD
misfit	5.61	5.62	5.52	5.59	5.77	5.90
H-Bond	-10.10	-10.07	-9.95	-12.66	-9.40	-12.21
vdW	-13.84	-13.83	-13.76	-14.01	-13.75	-13.83

**Table S4.** Selectivity of OFX ( $\alpha_{R-OFX/S-OFX}$ ) for each system (bars) and pH (circles), using the chiral selector CM- $\beta$ -CD at a 120-fold excess. Experiments were conducted at 25°C.

ES	Molar ratio	pH	$\alpha_{R-OFX/S-OFX}$	Error
L-menthol: C8 acid	(1:2)	4.8	1.19	0.03
L-menthol: C10 acid	(1:2)	4.6	1.42	0.04
L-menthol: C10 acid	(1:3)	4.5	1.85	0.05
L-menthol: C10 alcohol	(2:1)	6.3	0.92	0.04
L-menthol: C12 alcohol	(2:1)	6.2	0.97	0.08
C8 acid: C10 acid	(2:1)	4.5	1.43	0.03
C8 acid: C12 acid	(2:1)	4.6	1.60	0.03
C10 acid: C12 acid	(2:1)	4.4	2.01	0.06
C10 acid: C12 acid	(3:1)	4.7	1.34	0.04
C8 acid: C10 alcohol	(2:1)	4.7	1.26	0.05
C8 acid: C12 alcohol	(2:1)	5	1.12	0.04
C10 acid: C10 alcohol	(2:1)	4.5	1.36	0.04
C10 acid: C10 alcohol	(3:1)	4.5	1.5	0.03
C10 acid: C12 alcohol	(2:1)	5.3	1.31	0.04

**Table S5.** Experimental data of the selectivity of OFX ( $\alpha_{R-OFX/S-OFX}$ ) obtained through a central composite rotatable design, using C10 acid: C12 acid (2:1) as HES and CM- $\beta$ -CD as chiral selector.

Run	Real variables			$\alpha_{R-OFX/S-OFX}$
	pH	Excess of chiral selector	HES-water ratio (v/v)	
1	3.4	40	0.85	2.80
2	4.6	40	0.85	1.82
3	3.4	100	0.85	3.44
4	4.6	100	0.85	2.54
5	3.4	40	1.75	2.31
6	4.6	40	1.75	1.33
7	3.4	100	1.75	2.90
8	4.6	100	1.75	1.98
9	3	70	1.3	2.43
10	5	70	1.30	1.51
11	4	20	1.3	1.71
12	4	120	1.30	2.21
13	4	70	0.54	3.76
14	4	70	2.06	1.90
15	4	70	1.3	2.74
16	4	70	1.3	2.80
17	4	70	1.3	2.72
18	4	70	1.3	2.70
19	4	70	1.3	2.77
20	4	70	1.3	2.69

**Table S6.** Regression coefficients of the predicted second-order polynomial model for the selectivity of OFX ( $\alpha$ ) obtained from the central composite rotatable design,  $R^2 = 0.92$ .

	<b>Regression coefficients</b>	<b>Standard deviation</b>	<b>t-student (10)</b>	<b>p-value</b>
Mean	2.7446	0.1409	19.4755	0.0000
X <sub>1</sub>	-0.3628	0.0662	-5.4816	0.0009
X <sub>1</sub> <sup>2</sup>	-0.2500	0.0728	-3.4323	0.0110
X <sub>2</sub>	0.2011	0.0662	3.0391	0.0189
X <sub>2</sub> <sup>2</sup>	-0.2539	0.0728	-3.4861	0.0102
X <sub>3</sub>	-0.3906	0.0662	-5.9026	0.0006
X <sub>3</sub> <sup>2</sup>	0.0538	0.0728	0.7387	0.4841
X <sub>1</sub> X <sub>2</sub>	0.0989	0.0865	1.1437	0.2903
X <sub>1</sub> X <sub>3</sub>	0.0128	0.0865	0.1477	0.8867
X <sub>2</sub> X <sub>3</sub>	0.0069	0.0865	0.0802	0.9383

**Table S7.** ANOVA data for the selectivity of OFX ( $\alpha$ ) obtained from the central composite rotatable design.

	<b>SS</b>	<b>DF</b>	<b>Mean square</b>	<b>Fcal</b>	<b>p-value</b>	<b>Ftab</b>
<b>Regression</b>	6	5	1	24.3	<0.0001	3.20
<b>Residuals</b>	1	11	0			
<b>Fitting</b>	1	9	0	16.5	0.0585	19.38
<b>Pure error</b>	0	2	0			
<b>Total</b>	6	16				
<b>R<sup>2</sup> =</b>	0.92					

## Figures

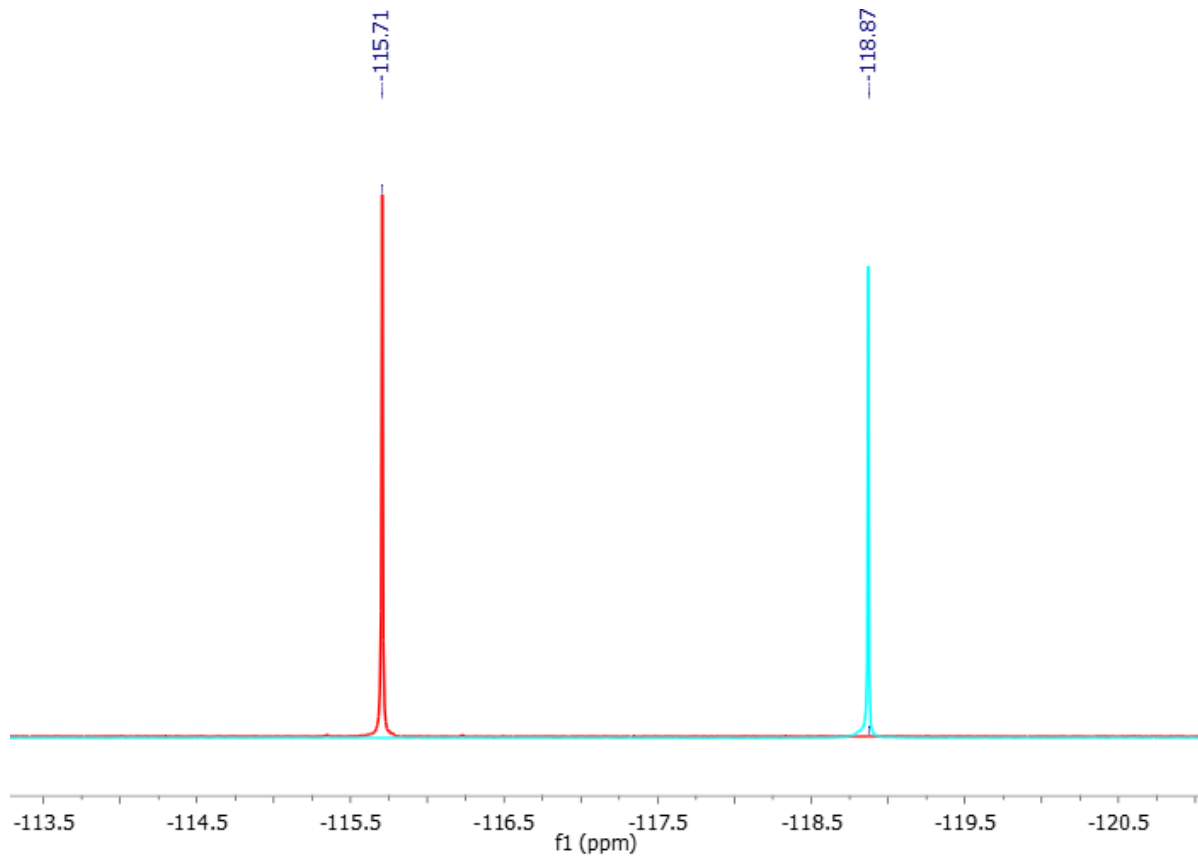


**Figure S1.** The  $^1\text{H}$ -decoupled  $^{19}\text{F}$  NMR spectrum of OFX (red) along with the  $^{19}\text{F}$  NMR spectrum of the internal standard (NaF, blue).

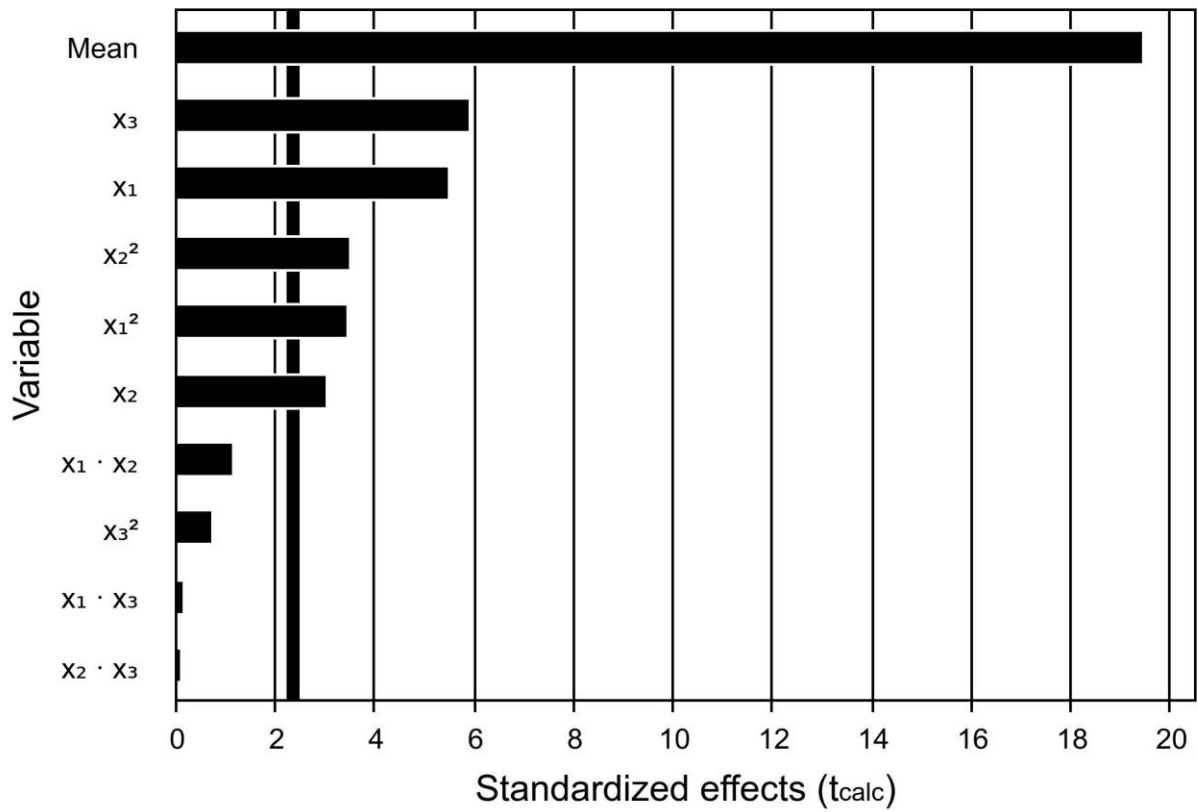


**Figure S2.** Pareto chart for the standardized main effects in the selectivity of OFX ( $\alpha$ ), with 95% of confidence.



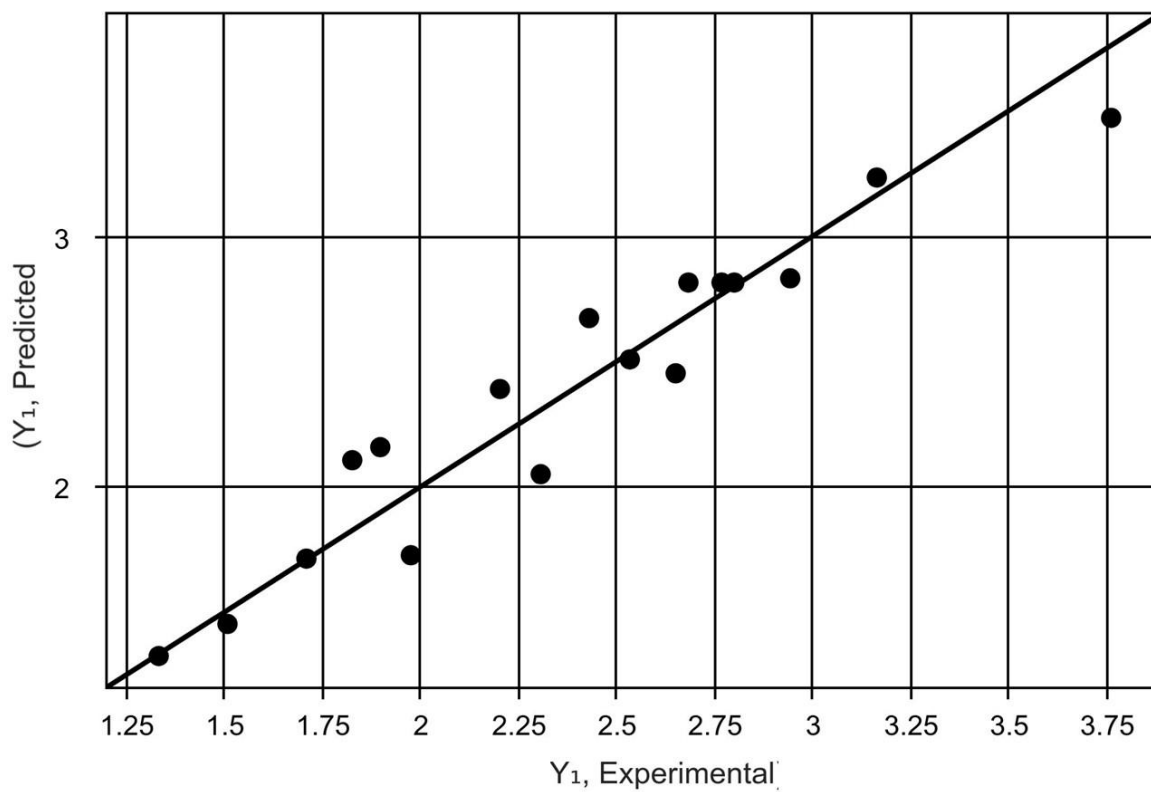


**Figure S3.** Predict vs. observed values of the selectivity of OFX ( $\alpha$ ).